Title
COHERENT K* PRODUCTION IN THE K+d REACTION AT 2.3 BeV/c

Authors
Butterworth, Ian
Brown, John L.
Goldhaber, Gerson
et al.

Publication Date
1965-08-02

UCRL-16300

University of California

Ernest O. Lawrence Radiation Laboratory

COHERENT K^* PRODUCTION IN THE K^+d REACTION AT 2.3 BeV/c

Berkeley, California

Submitted to Phys. Rev. Letters UCRL-16300

UNIVERSITY OF CALIFORNIA
Lawrence Radiation Laboratory
Berkeley, California

AEC Contract No. W-7405-eng-48

COHERENT K^* PRODUCTION IN THE K^+d REACTION AT 2.3 BeV/c

Ian Butterworth, John L. Brown, Gerson Goldhaber,
Sulamith Goldhaber, Allan A. Hirata, John A. Kadyk,
and George H. Trilling

August 2, 1965

Coherent K^* Production in the K^+d Reaction at 2.3 BeV/c*

Ian Butterworth, John L. Brown, Gerson Goldhaber, Sulamith Goldhaber, Allan A. Hirata, John A. Kadyk, and George H. Trilling

Department of Physics and Lawrence Radiation Laboratory
University of California, Berkeley, California

August 2, 1965

In a study of K^+d interactions at 2.3 BeV/c we have observed the following reactions with single and double pion production in which the deuteron does not break up:

$$K^+d \rightarrow K^0 \pi^+ d \qquad (1)$$

$$K^+d \rightarrow K^+ \pi^- \pi^+ d. \qquad (2)$$

These reactions proceed almost entirely through K^* production. We further note a broad enhancement in the π^+d mass distribution in reaction (2) which we interpret to be the result of N^{*++} production without deuteron breakup, i.e., $(d\pi^+) = (N^{*++}n)$. We will show that one can interpret our results in terms of coherent K^* production on the deuteron, the survival of which in the final state imposes a strong restriction on the maximum possible momentum that can be transferred to it. The deuteron thus acts effectively like a "momentum-transfer filter".

The work described here is based on an analysis of 100 000 pictures taken with the BNL 20-in. bubble chamber filled with deuterium and exposed in a 2.3-BeV/c K^+ meson beam at the AGS.[1]

The events assigned to reaction (1), for which we only included the charged K^0 decay mode, and to reaction (2) were identified by applying four-constraint kinematical fits as well as ionization estimates on the scanning table.[2]

We have observed 33 events of reaction (1) and 81 of reaction (2), respectively amounting to $(2.8 \pm 0.8)\%$ and $(4.2 \pm 0.7)\%$ of the corresponding reactions with deuteron breakup. The observed events yield cross sections of $(150 \pm 35)\ \mu b$ and $(110 \pm 16)\ \mu b$ for reactions (1) and (2) respectively.[3] The properties of the two reactions will now be discussed in turn.

The Dalitz plot of $M^2_{d\pi^+}$ vs $M^2_{K^0\pi^+}$ for reaction (1) is shown in Fig. 1a. It is seen that the reaction goes almost exclusively through the channel $K^+d \to K^{*+}d$. There is no evidence for any structure in the $d\pi^+$ mass distribution.

We have carried out an approximate calculation to test whether the differential cross section for K^* production agrees with the impulse approximation where one combines free-nucleon amplitudes and neglects binding energy and double-scattering effects. On a peripheral single-meson exchange model for K^* production, the nucleon amplitudes are given by the sum of the isoscalar and isovector exchange amplitudes. In the deuteron, however, the isovector amplitudes from the neutron and proton cancel, leaving only the isoscalar exchange which is the same for neutron and proton. Hence, summing over spin states, we obtain

$$\left(\frac{d\sigma}{d\Delta^2}\right)_d = 4\left[\left(\frac{d\sigma}{d\Delta^2}\right) + 2/3\left(\frac{d\sigma}{d\Delta^2}\right)'\right]\left|\frac{F(q)}{F(0)}\right|^2 . \qquad (3)$$

Here $(d\sigma/d\Delta^2)$ and $(d\sigma/d\Delta^2)'$ are the cross sections one would have for purely isoscalar exchange with a nucleon involving no spin flip and spin flip respectively, $F(q)$ is the Fourier transform of the square of the deuteron radial wave function and q is the momentum transfer to the deuteron.[4] Of course, we do not have direct access to these cross sections, and therefore they have been obtained by a fairly crude estimate from the available experimental data.[5-8] In Fig. 1b we show the observed differential cross section compared with the results of the calculation. In view of the approximations made, the results of the calculation agree reasonably well with the data, suggesting that the application of the impulse approximation is basically correct.

Absence of events reflecting the nucleon amplitudes for the reaction $Kp \to N^*K$ results from the low momentum transfer to the deuteron. An artificial imposition of such a momentum-transfer cutoff to events where the deuteron breaks up, i. e., $K^*d \to K^0\pi^+pn$, suppresses the N^* production events similarly.

Turning to reaction (2) we note that the dominant feature is again K^* production. However, we also observe enhancements at low $d\pi^+$ masses and at low $K\pi\pi$ masses. Figure 2a shows the phase-space triangle of $M_{d\pi^+}$ vs $M_{K^+\pi^-}$, with the respective mass projections. Reaction (2) appears to proceed principally through pseudoscalar meson exchange between the K^* and π^+d vertex (see inset to Fig. 3). The evidence for this process is demonstrated for K^* events in Fig. 3a, where we show that the $K\pi$ scattering angle, α_{K^*}, follows a $\cos^2\alpha_{K^*}$ distribution.

Such a model allows interpretation of all the dominant features of the reaction as follows. The peaking at low masses of the $K\pi\pi$ system may be understood from the low momentum transfer to the deuteron (and hence to the $K\pi\pi$ system) imposed by the deuteron form factor. Figure 4a shows the Chew-Low plot of momentum transfer to the $K\pi\pi$ system against its squared mass, together with projections. The curve shown on the Δ^2 projection has again been calculated using the cross sections for the corresponding K^+p reactions.[9,10] The lower limits on the four-momentum transfer imposed by the Chew-Low boundary have not been taken into account here. This gives rise to the deviations from the data at low Δ^2 values. On examining Fig. 4a it becomes evident that the observed enhancement at low $K\pi\pi$ masses can be explained by the kinematics of the reaction in conjunction with the low Δ^2 filter imposed by the deuteron.

Figure 4b shows the Chew-Low plot for the $d\pi^+$ system for events where $M_{K^+\pi^-}$ is in the K^* region. The rapid fall-back of the kinematic boundary will again produce an enhancement at low $d\pi^+$ masses in view of the relatively small values of momentum transfer. Furthermore, one expects a broad peaking at low $d\pi^+$ masses as a consequence of N^* formation between the π^+ and the proton of the deuteron, with subsequent recombination of the decay proton from the N^* with the spectator neutron.[11, 12] Events where the deuteron breaks up, i.e., $K^+d \rightarrow K^+\pi^-\pi^+pn$, show a $pn\pi^+$ mass distribution very similar to the observed $d\pi^+$ distribution if a low momentum transfer to the pn system is artificially imposed. Evidence for presence of several angular-momentum states in the $d\pi^+$ system is presented in Fig. 3b, which shows a strong forward peaking in $\cos\alpha_{d\pi^+}$. Here $\alpha_{d\pi^+}$ is the scattering angle in the $d\pi$ center of mass. This observation favors the above interpretation of the π^+d enhancement over that of a fundamental $d\pi$ resonance, where we expect a unique angular momentum to be present.

Recently, similar effects to those reported here for reaction (2) have been observed in π^-d experiments at 3.7 BeV/c[13] and 3.2 BeV/c[14], where the ρ^0 is formed in place of the K^{*0}.

We would like to acknowledge helpful discussions with A. S. Goldhaber. We are grateful to R. Shutt and his co-workers at the Brookhaven National Laboratory for making available the 20-in. bubble chamber, to the AGS crew, the 20-in. bubble chamber crew, and particularly to H. Brown for help with the exposure at the AGS. Of the many people who helped with scanning, measuring, and computing, we would like particularly to thank D. Armstrong, J. Gutierrez, W. S. Little, and F. S. Sieh. Finally we wish to acknowledge the help of B. C. Shen in various stages of this work.

FOOTNOTES AND REFERENCES

*This work was done under the auspices of the U. S. Atomic Energy Commission.

1. C. Baltay, J. Sandweiss, J. Sanford, H. Brown, M. Webster, and S. Yamamoto, Nucl. Instr. Methods 20, 37 (1963).

2. If the events with a deuteron in the final state are fitted to the hypotheses $K^+d \to K^0\pi^+pn$ and $K^+d \to K^+\pi^-\pi^+pn$, they yield a clear "spike" at the lower limit of the pn effective-mass distribution. Of course, in fitting to these hypotheses an event with a deuteron as a product, the deuteron recoil is misidentified as a proton. The momentum deduced from the range of the "proton" is thus somewhat larger than, but very nearly equal to, half the deuteron momentum. Thus a valid fit is obtained with the proton and neutron having essentially the same momentum and so yielding the minimum pn effective mass.

3. In finding cross sections, we have corrected for unseen K^0 decays and for loss of short-range deuterons. Ambiguous events (~5 in each channel) have been allowed for in the errors but have not been included in the analysis.

4. M. Gourdin and A. Martin, Nuovo Cimento 11, 670 (1959).

5. In this calculation we assume that the quantity in the square bracket of (3) can be replaced by the overall isoscalar contribution to the reaction $K^+p \to K^*p$, i.e., the factor 2/3 is approximated by 1. The isoscalar contribution is estimated as follows: The reaction $K^+p \to K^*p$ is well known to involve both vector and pseudoscalar exchange at low energies, with the former predominating as the

energy rises and being essentially the only component at 3 BeV/c (Ref. 6). We have shown elsewhere that the vector exchange is the isoscalar component (Ref. 7). Therefore the shape of the isoscalar differential cross section was taken from the 3-BeV/c data, and its magnitude was obtained by interpolation between the total K^* production cross section at 3 BeV/c and the estimate of the vector-exchange part of the cross section at 1.96 BeV/c (Ref. 8).

6. M. Ferro-Luzzi, R. George, Y. Goldschmidt-Clermont, V. P. Henri, B. Longejans, D. W. G. Leith, G. R. Lynch, F. Muller, and J. M. Perreau, Nouvo Cimento 36, 1101 (1965).

7. S. Goldhaber, I. Butterworth, G. Goldhaber, A. H. Hirata, J. A. Kadyk, T. A. O'Halloran, B. C. Shen, and G. H. Trilling, presented at the International Conference on High Energy Physics, Dubna, 1964 (unpublished); Lawrence Radiation Laboratory Report UCRL-11465, July 1964 (unpublished).

8. S. Goldhaber, in Proceedings of the Athens Conference on Recently Discovered Particles (Ohio University Press, Athens, Ohio, 1963), p. 92.

9. The reaction $K^+p \rightarrow K^*p\pi^+$ goes predominantly by pion exchange, with the $p\pi^+$ system forming the $N^*(1238)$ resonance. Since the K^* in this reaction is assumed to be produced by pion exchange, we argue that the momentum transfer to the deuteron may be approximated by that to the proton in the K^+p reaction modified by the factor $|F(q)/F(0)|^2$. The contribution of the neutron at the π^+n vertex is small and is neglected. The overall K^* production cross section in the reaction $K^+p \rightarrow K^*p\pi^+$ is, within errors, the same at 1.96 BeV/c and 3 BeV/c (Refs. 6 and 10). The differential cross section

for 1.96 BeV/c has been employed for the estimate discussed in the text.

10. G. Goldhaber, W. Chinowsky, S. Goldhaber, W. Lee, and T. O'Halloran, Phys. Letters 6, 62 (1963).

11. A. Ramakrishnan, V. Devanathan, and K. Venkatesan, Nucl. Phys. 29, 680 (1962).

12. S. Mandelstam, Proc. Roy. Soc. (London) A244, 491 (1958).

13. M. A. Abolins, D. D. Carmony, R. L. Lander, and Ng. -h Xuong, Phys. Rev. Letters 15, 125 (1965).

14. L. Seidlitz, O. I. Dahl, and D. H. Miller, Lawrence Radiation Laboratory, (private communication).

FIGURE LEGENDS

Fig. 1. The reaction $K^+d \to K^0\pi^+d$. (a) Dalitz plot of $M^2_{d\pi^+}$ vs $M^2_{K^0\pi^+}$ with projections; (b) four-momentum transfer distribution to the $K^0\pi^+$ system (or to the deuteron). The solid curve results from the calculation discussed in the text.

Fig. 2. $M_{d\pi^+}$ vs $M_{K^+\pi^-}$ for the reaction $K^+d \to K^+\pi^-\pi^+d$, with projections. For the $M_{d\pi^+}$ projection the shaded histogram shows the distribution for events with $M_{K^0\pi^+}$ in the K^* region (0.84 to 0.96 BeV). The solid and dashed curves show phase space for $Kd \to K\pi\pi d$ and $Kd \to K^*\pi d$, respectively, normalized to the appropriate number of events.

Fig. 3. The reaction $K^+d \to K^+\pi^-\pi^+d$. (a) Distribution of $\cos\alpha_{K^*} = (|\underset{\sim}{K}_{in} \cdot \underset{\sim}{K}_{out}|)/(|\underset{\sim}{K}_{in}||\underset{\sim}{K}_{out}|)$, the cosine of the $K\pi$ scattering angle in the $K\pi$ center of mass, for events with $0.84 \leq M_{K\pi} \leq 0.96$ BeV. (b) Distribution of $\cos\alpha_{d\pi^+} = (|\underset{\sim}{d}_{in} \cdot \underset{\sim}{d}_{out}|)/(|\underset{\sim}{d}_{in}||\underset{\sim}{d}_{out}|)$, the cosine of the $d\pi^+$ scattering angle in the $d\pi^+$ center of mass, for events with $2.01 \leq M_{d\pi^+} \leq 2.3$ BeV.

Fig. 4. The reaction $K^+d \to K^+\pi^-\pi^+d$. (a) Chew-Low plot of $\Delta^2_{K\pi\pi}$ vs $M^2_{K\pi\pi}$. The solid points are for events with $0.84 < M_{K^+\pi^-} < 0.96$ BeV, i.e., in the K^* region. Those marked x are for events outside this region. Shaded histograms refer to the former events. The smooth curve on the $M^2_{K\pi\pi}$ projection shows phase space for $Kd \to K\pi\pi d$, the dotted curve that for $Kd \to K^*\pi d$. The curve on the momentum-transfer distribution shows the result of the calculation described in the text. The dotted line joining the two projections shows that $M^2_{K\pi\pi}$ would have to be less than 1.8 BeV^2 if the "momentum-transfer

filter" produced by the deuteron form factor were approximated by a sharp cutoff at 0.2 BeV^2. (b) Chew-Low plot of $\Delta^2_{d\pi}$ vs $M^2_{d\pi}$ for events with $0.84 < M_{K^+\pi^-} < 0.96$ BeV.

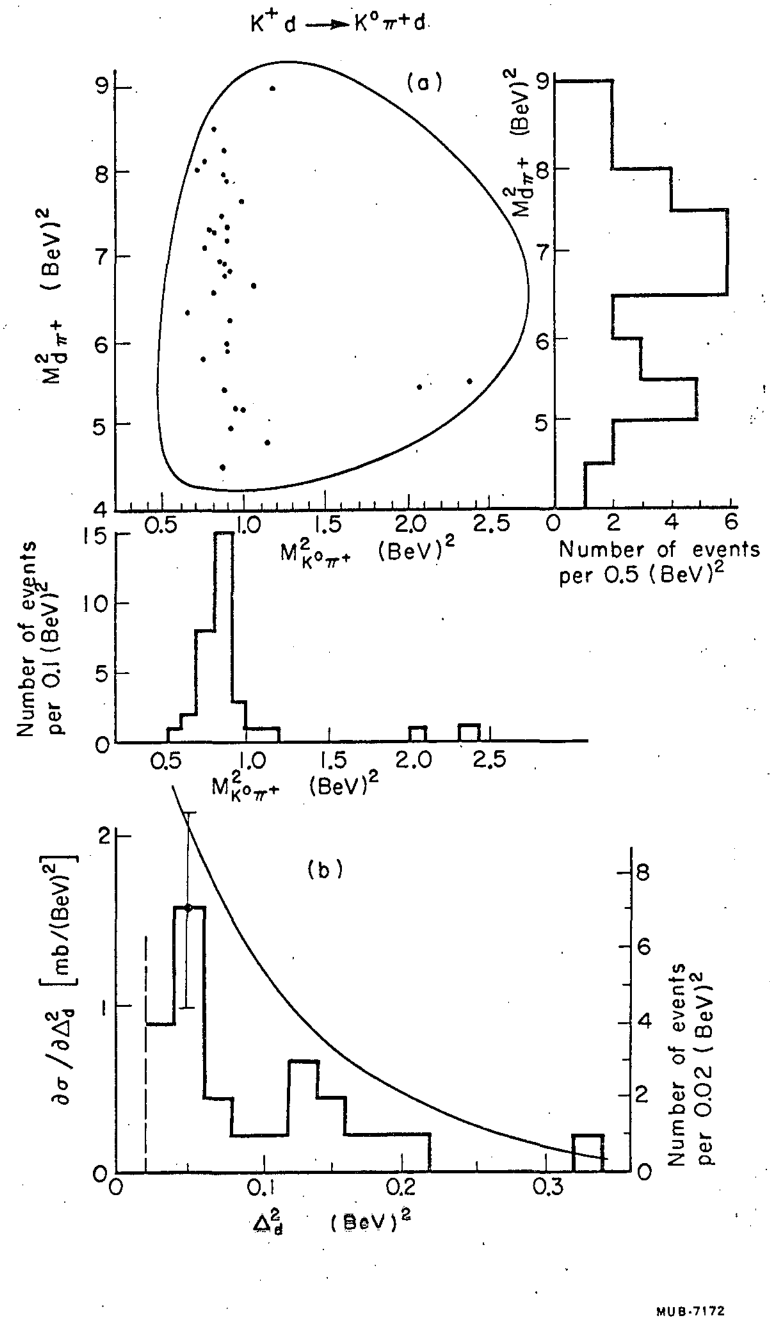
$K^+d \rightarrow K^o\pi^+d$
(a)
$M^2_{d\pi^+}$ (BeV)^2
$M^2_{K^o\pi^+}$ (BeV)^2
Number of events per 0.5 (BeV)^2
Number of events per 0.1 (BeV)^2
(b)
$\partial\sigma/\partial\Delta^2_d$ [mb/(BeV)^2]
Number of events per 0.02 (BeV)^2
Δ^2_d (BeV)^2
MUB-7172

Fig. 1

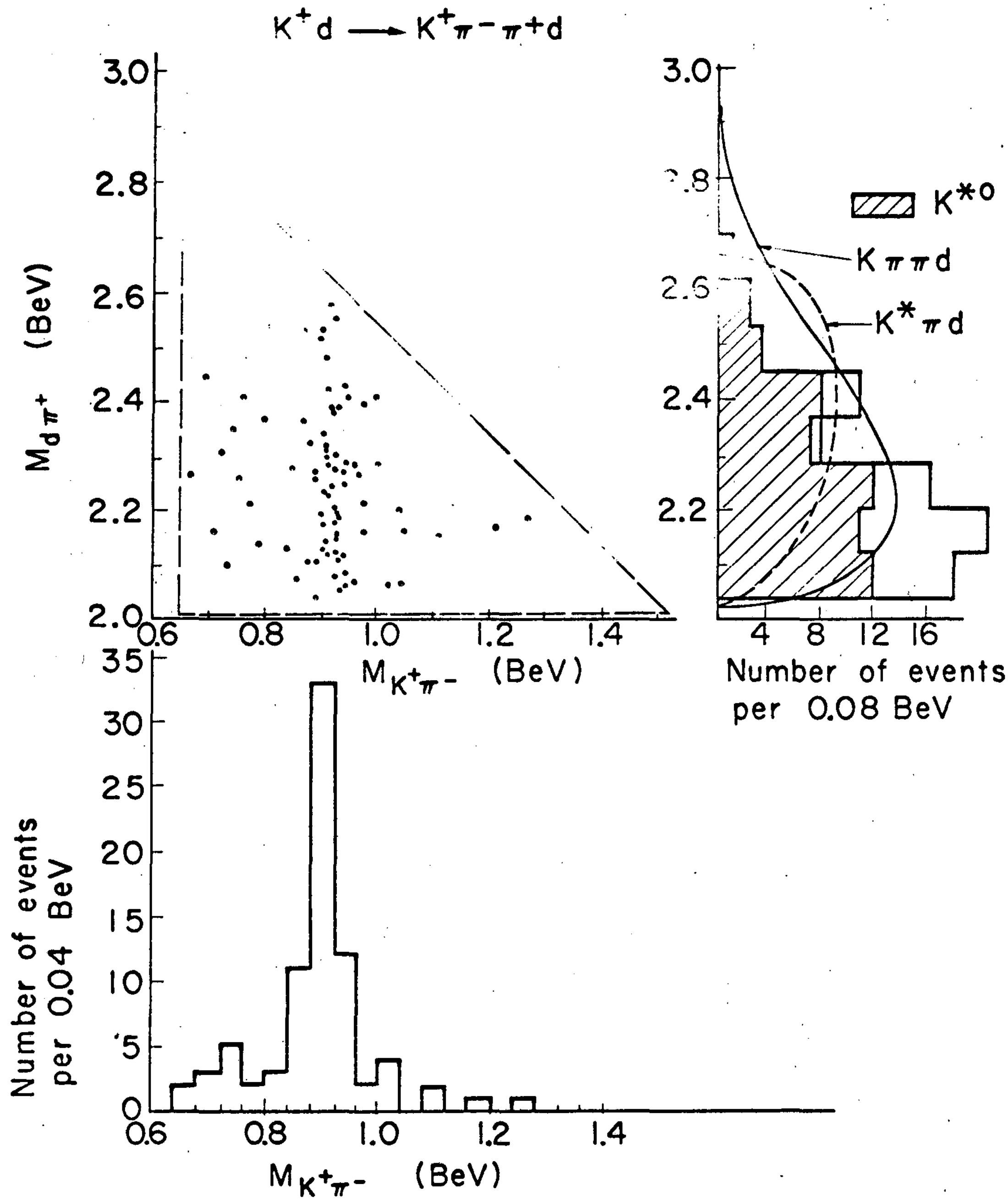
K⁺d ⟶ K⁺π⁻π⁺d
K*0
Kππd
K*πd
M_{dπ⁺} (BeV)
M_{K⁺π⁻} (BeV)
Number of events per 0.08 BeV
Number of events per 0.04 BeV
MUB-7173

Fig. 2

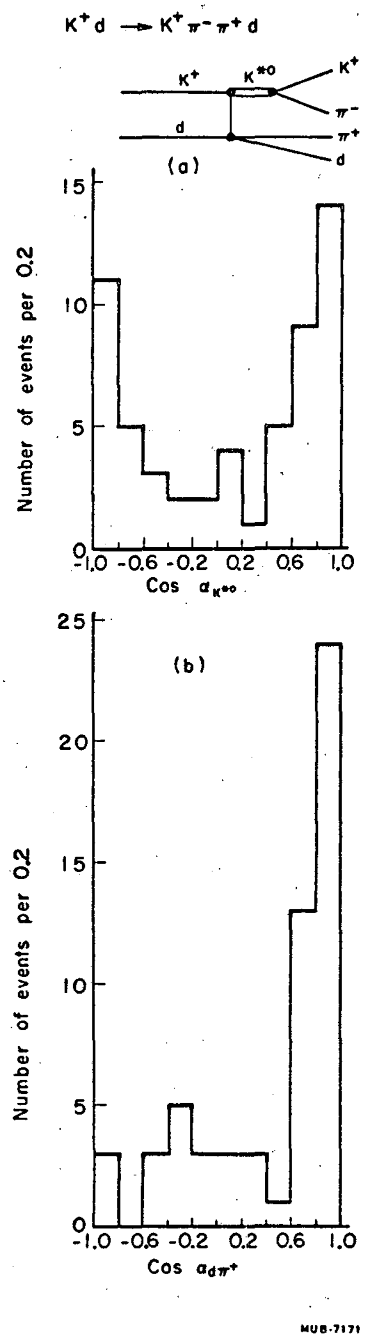
$K^+d \rightarrow K^+\pi^-\pi^+d$
K^+
K^{*0}
K^+
π^-
d
π^+
d
(a)
Number of events per 0.2
Cos $\alpha_{K^{*0}}$
(b)
Number of events per 0.2
Cos $\alpha_{d\pi^+}$
MUB-7171

Fig. 3

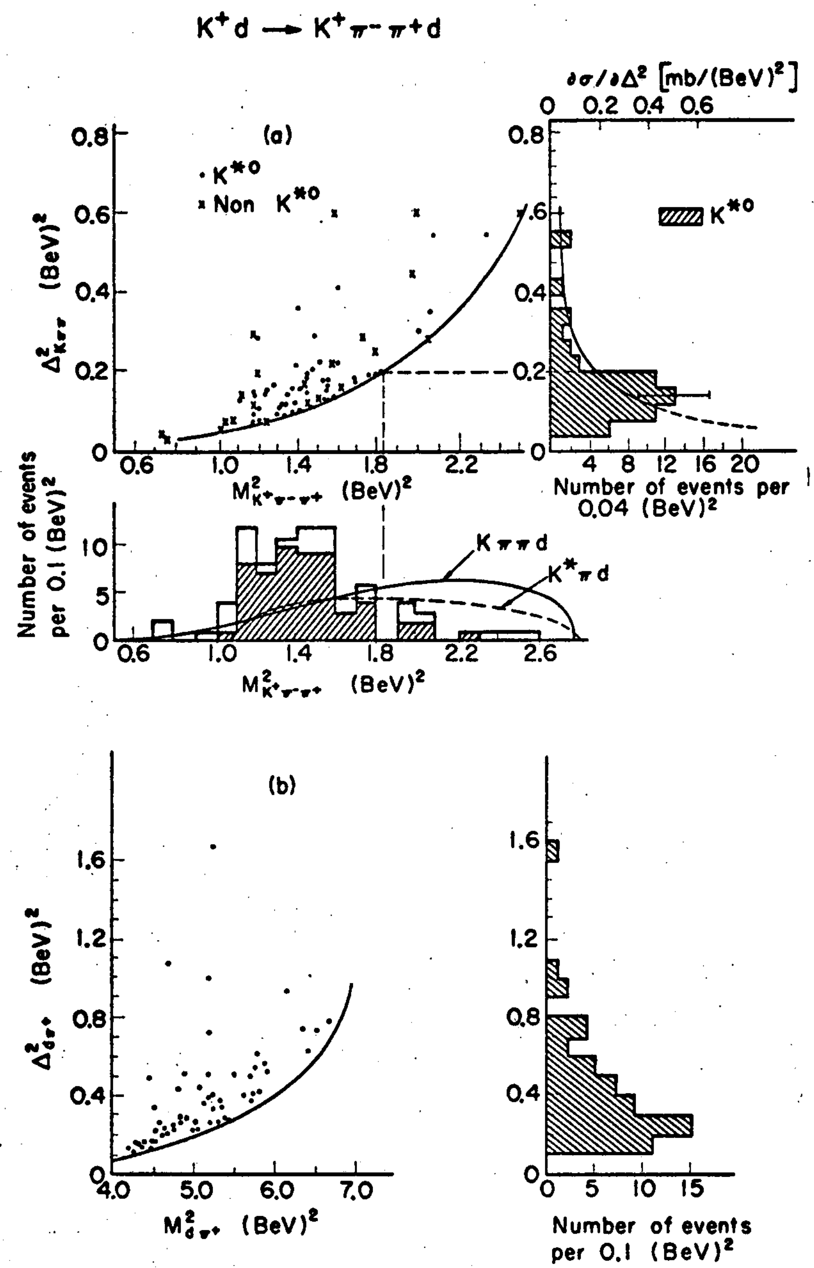
K+d → K+π−π+d
(a)
• K*0
x Non K*0
K*0
dσ/dΔ² [mb/(BeV)²]
0 0.2 0.4 0.6
0.8
0.6
0.4
0.2
0
Δ²Kππ (BeV)²
0.6 1.0 1.4 1.8 2.2
M²K+π−π+ (BeV)²
4 8 12 16 20
Number of events per 0.04 (BeV)²
Number of events per 0.1 (BeV)²
10
5
Kππd
K*πd
0.6 1.0 1.4 1.8 2.2 2.6
M²K+π−π+ (BeV)²
(b)
1.6
1.2
0.8
0.4
0
Δ²dπ+ (BeV)²
4.0 5.0 6.0 7.0
M²dπ+ (BeV)²
0 5 10 15
Number of events per 0.1 (BeV)²

Fig. 4